Karatzia, X. A., Mylonakis, G. E., & Bouckovalas, G. D. (2017). Equivalent-linear dynamic stiffness of surface footings on liquefiable soil. In *COMPDYN 2017 - Proceedings of the 6th International Conference on Computational Methods in Structural Dynamics and Earthquake Engineering* (pp. 1388-1402). National Technical University of Athens. https://doi.org/10.7712/120117.5500.18213

COMPDYN 2017
6th ECCOMAS Thematic Conference on
Computational Methods in Structural Dynamics and Earthquake Engineering
M. Papadrakakis, M. Fragiadakis (eds.)
Rhodes Island, Greece, 15–17 June 2017

EQUIVALENT-LINEAR DYNAMIC STIFFNESS OF SURFACE FOOTINGS ON LIQUEFIABLE SOIL

Xenia A. Karatzia[1], **George E. Mylonakis**[1,2], **and George D. Bouckovalas**[3]

[1] University of Patras
Dept. of Civil Engineering, Rio 26500, Greece
{xkar, mylo}@upatras.gr

[2] University of Bristol
Dept. of Civil Engineering, Queens Building, Bristol BS8 1TR, U.K.
g.mylonakis@bristol.ac.uk

[3] NTUA
School of Civil Engineering, Iroon Polytechniou 9, Zografou 15780, Greece
gbouck@central.ntua.gr

Keywords: Equivalent-Linear, Static Stiffness, Liquefiable Soil, Surface Footing, Three-Layer Soil Profile.

Abstract. *The focus of the present study is upon the influence of liquefaction on the dynamic impedance (stiffness and damping) of rigid square footings resting on liquefiable soil under external harmonic loading. A three-layer soil profile, consisting of a loose liquefiable sandy layer sandwiched between two impermeable stiff clayey layers, is considered to this end. Using simplified cone models and rigorous boundary element analyses, a systematic parametric study is performed to investigate the influence of liquefaction on the dynamic impedance of the footing. Vertical, horizontal and rocking oscillations are considered in the frequency domain. The results demonstrate that for common soil, foundation and seismic excitation conditions, liquefaction in the foundation soil yields significant degradation of the dynamic spring coefficients and increases the associated damping coefficients. Based on the parametric study, regression formulae are obtained for estimating the static stiffness coefficient of rigid square footings on liquefied soil.*

1 INTRODUCTION

Contrary to the current engineering practice, which dictates the use of deep foundations in soils prone to liquefaction, new evidence suggests also the use of shallow foundations provided the existence of a non-liquefiable soil layer on top of the liquefiable layer is appropriately considered. If this non-liquefiable surface "crust" exhibits adequate thickness and shear strength, it can prevent the seismic settlement accumulation and post-shaking bearing capacity failure. Recently, Karamitros et al [1-3] have developed a design approach for the performance-based design of shallow foundations on liquefiable soils. The design is based on the idea of a natural or artificial crust, which needs not extend over the whole depth of the liquefiable sand, in order to take advantage of the observed benefits of settlement reduction [4-5], as well as the seismic motion attenuation ("natural seismic isolation") due to the liquefiable soil below the crust. Within the above context the need arises to investigate the dynamic response of shallow foundations on liquefiable soils.

The study of dynamic stiffness and damping of a footing on a liquefiable soil profile is a complex and intricate problem, mainly due to the complexity and nonlinearity of the liquefaction phenomenon itself. Despite extensive research during the last decades, the mechanisms of seismic wave propagation within the liquefied soil are mostly unidentified. It is known that shear-induced dilation under extremely low effective stresses leads to a significant variation in excess pore pressure and in seismic wave propagation velocity even within the same loading cycle. As a result, the mechanical properties of liquefied soil are time-variant during the seismic excitation rendering the problem extremely difficult to analyze. Additionally, the gradual pore pressure dissipation may induce important settlements and detachment of the foundation from the ground. Yet, another difficulty in handling the dynamic impedance problem arises from the existence of a multilayer soil profile (at least three-layer soil, i.e., non liquefiable surface layer – liquefiable soil layer – non liquefiable base stratum) with sharp impedance contrast between the soil layers, which results in strong wave reflections and entrapment of seismic energy within the middle liquefiable soil layer.

On the other hand, the available solutions regarding the dynamic impedance of footings on non-liquefiable soil usually assume linear or equivalent-linear elastic soil behavior and perfect contact between footing and soil [6-14]. Moreover, soil-foundation interaction is approached by means of an equivalent spring-dashpot system connected with the footing, as shown in Fig. 1a. These formulations are usually rigorous, as the stiffness and damping coefficients are obtained from exact numerical solutions of the corresponding boundary value problems. Evidently, such solutions cannot be implemented in the case of a footing on liquefiable soil.

The scope of this paper is to investigate the dynamic stiffness and damping of a rigid surface square footing resting on liquefiable soil, under external harmonic loading. To this end, the simplest case of a three-layer soil profile consisting of a liquefiable sandy soil layer sandwiched between two stiff cohesive soil layers is considered. For the exploration of the problem, equivalent-linear elastic analyses are utilized, in conjunction with appropriate values for the material constants of liquefied soil. Recent experimental and analytical evidence suggest that during the course of liquefaction, the shear wave propagation velocity can be reduced to 10 – 30% of its initial value [15-16] and the soil material damping ratio may increase to over 20%, in agreement with a substantial increase in imposed shear strains.

These observations allow for a simplification of the problem, which can be separated into two different phases: a) the initial phase (pre-liquefaction) and b) the phase during liquefaction (post-liquefaction) with the material properties of the liquefied soil properly adjusted over those prior to liquefaction. It is further assumed that there is no sufficient soil permeability above and below the liquefied layer so that the change in soil stiffness and damping may

be viewed as "permanent" during liquefaction. This is certainly a simplification, but can be considered realistic for the purposes of an earthquake dynamic analysis. Through this decomposition and the simplifying assumptions, one may analyze each phase separately by means of equivalent-linear analysis.

2 PROBLEM DEFINITION

Fig. 1b depicts the problem under investigation: a rigid square ($B\times B$) surface footing on a liquefiable soil profile subjected to harmonic loading. A three-layer soil profile, including a surface clayey crust over a loose sandy liquefiable layer followed by a stiff base clayey stratum, is assumed. The dynamic impedance functions of the footing are obtained for three oscillation modes (vertical, horizontal and rocking). Numerical analyses refer to square footings of various sizes used for the foundation of both ordinary structures and bridge piers. Excitation frequencies cover the frequency range of importance in earthquake engineering.

To examine the influence of liquefaction on the spring and dashpot coefficients, elastodynamic analyses are conducted for both phases, prior and post liquefaction. For post-liquefaction conditions, it is assumed that the shear wave propagation velocity of the middle liquefiable soil is reduced to about 17% of its initial value, i.e., from V_{s2} = 150 m/s decreases to V_{sliq} = 25m/s. In view of the increase in energy loss due to material damping during liquefaction, in the present analyses the material damping ratio in the middle soil stratum is assumed to be equal to β_2 = 3% without liquefaction and equal to β_{liq} = 20% in presence of liquefaction. Given the impermeable nature of the layers above and below the liquefied zone, no pore water pressure dissipation effects are considered. The soil below the surface layer is considered fully saturated and, hence, a uniform value for Poisson's ratio ν = 0.49 is employed corresponding to a nearly incompressible medium.

Unless otherwise specified, the material properties of the surface layer employed in the following analyses are shear wave propagation velocity V_{s1} = 100, 250 m/s, Poisson's ratio ν_1 = 0.33, material damping ratio β_1 = 3%, mass density ρ_1 = 2 Mg/m^3. The properties of the middle liquefiable layer are V_{s2} = 150 m/s, ν_2 = 0.49, β_2 = 3%, ρ_2 = 2 Mg/m^3 and the properties of the base stratum are V_{s3} = 300 m/s, ν_3 = 0.49, β_3 = 3%, ρ_3 = 2 Mg/m^3. With reference to the thicknesses of the surface crust and the liquefiable soil layer, three values are evaluated h_1/B = 0.5, 1, 2 and h_2/B = 0.5, 1, 2. The total thickness of the soil profile equals $H/B \cong 15$, thus, the presence of bedrock does not affect the dynamic response of the footing. Accordingly, the parametric investigation is focused upon the effect of the thickness of the liquefied stratum, as well as the thickness and stiffness of the non-liquefiable surface crust (which should meet the bearing capacity and settlement requirements under gravity loading).

To obtain a set of governing problem parameters, dimensional analysis was employed. The problem involves six major dimensional independent parameters (M = 6): the thickness of surface crust, h_1, the thickness of liquefiable layer, h_2, the shear wave propagation velocity of non-liquefiable surface crust, V_{s1}, the corresponding velocity of liquefiable layer, V_{s2}, the footing width, B, and the excitation frequency, f. The rest of parameters illustrated in Fig. 1b, including the stiffness of the base layer and the total thickness of the soil profile, are of rather minor importance (i.e. have a second order influence on the response) and are not explored parametrically in the ensuing.

In light of the two fundamental dimensions, length [L] and time [T] (N = 2), application of Buckingham's theorem [17] ($M - N$ = 4) yields four dimensionless ratios controlling the response of the footing. The governing dimensionless groups were selected to be h_1/B, h_2/B, V_{s1}/V_{s2}, $\omega h_1/V_{s1}$. These ratios can describe adequately the dynamic response of the footing.

Therefore, a parametric study is performed to identify the influence of the aforementioned parameters on the dynamic stiffness and damping of the footing.

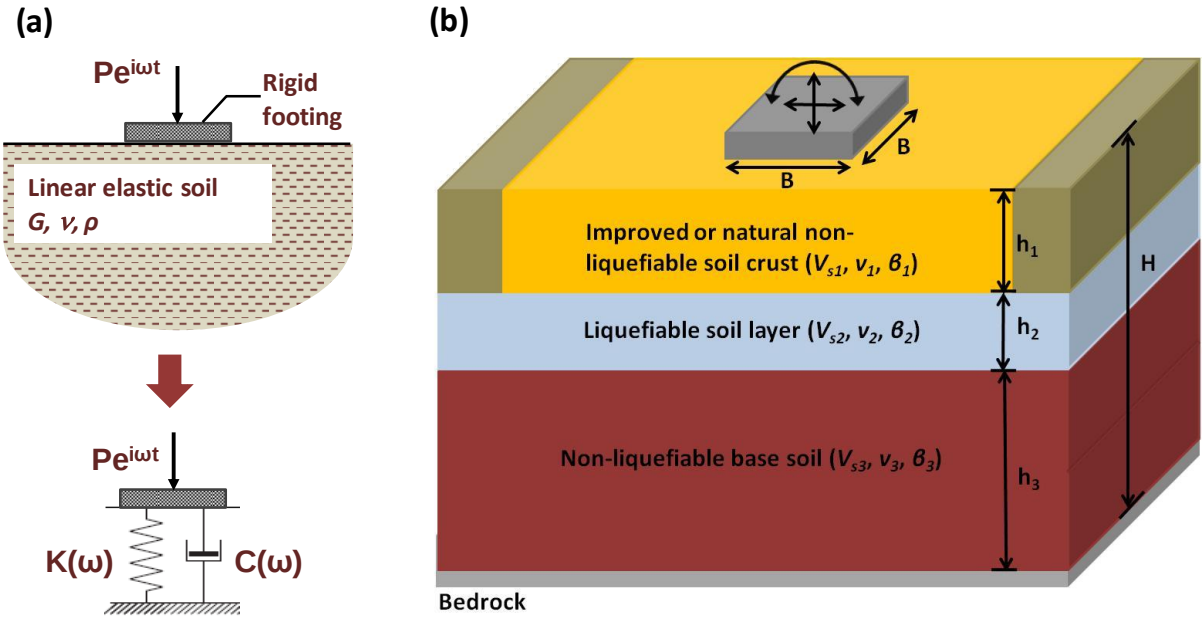

Figure 1: a) Modeling of soil-foundation interaction, b) Problem definition and main parameters involved

3 METHOD OF ANALYSIS

3.1 Numerical modeling tools

The dynamic impedance problem of the foundation on liquefiable soil is analyzed using Cone model solutions. Namely, Wolf and Deeks [18] used wave propagation in cones in order to develop a methodology for determining the dynamic stiffness and damping of surface or embedded cylindrical rigid foundations. Translational and rotational truncated cones (conical bars) are based on Strength-of-Materials theory, following the assumption of "plane sections remain plane" with the associated one-dimensional displacements. By means of cone models, the complex three-dimensional elastodynamic problem is simplified to a problem of one-dimensional wave propagation, which admits an exact solution. Apart from cylindrical foundations, various foundation shapes can be analyzed by considering an equivalent circular radius to match footing area for translational oscillation modes ($R = B/\sqrt{\pi}$), or moment of inertia for rotational oscillation modes ($R = B/\sqrt[4]{(3\pi)}$). A multilayer soil profile overlying a half-space or bedrock may be readily employed, consisting of any number of horizontal layers with linear elastic behavior and hysteretic material damping. Dynamic stiffness and damping are evaluated for any single frequency for vertical, horizontal, rocking and torsional degrees of freedom. This *strength-of-materials approach to foundation dynamics* was implemented in the commercial computer code CONAN [18]. The accuracy of the cone model predictions has been verified in a number of studies, which indicate that the deviation in impedance functions between cone solution and the rigorous solutions is within ± 20% [18-19].

To perform a systematic, more accurate and in-depth analysis of the problem at hand, a rigorous Boundary Element Method in 3 dimensions implemented in software platform ISo-BEM [20] is also employed. In the BEM formulation, the multilayer medium is solved by considering each soil stratum as a separate homogeneous region, developing BEM equations

independently and then assembling and solving the associated set of simultaneous equations by respecting equilibrium and compatibility across a common interface. BEM allows for the reduction in the dimensionality of the problem (from 3D to 2D) which means that only surfaces are discretized. In these analyses, isoparametric four-noded linear quadrilateral elements are used for meshing the surfaces. Note that ISoBEM has been successfully used to study several problems of applied mechanics [21-22] and soil mechanics [23]. Three-dimensional models simulating a rigid square footing on a three-layer liquefiable soil in ISoBEM were set up with a dual purpose: a) to provide comparisons and b) to yield fitted formulae for static stiffness.

3.2 Elastic dynamic impedance

For static conditions, the stiffness of a rigid foundation assuming linear or equivalent-linear soil is expressed by the following dimensionally consistent form

$$\frac{K_{ij}^{0}}{G\,B^{m}} = f_{ij}(\nu) \tag{1}$$

where K^0_{ij} denotes the force or moment along the degree of freedom i for a unit displacement or rotation along the degree of freedom j; G denotes the soil shear modulus and B the foundation width. The exponent m admits 1 for the translational and 3 for the rotational degrees of freedom. $f_{ij}\ (\nu)$ is a dimensionless factor dependent solely on Poisson's ratio. Given that this work deals with surface footings, the coupling term has been omitted and only the vertical (K^0_{vv}), horizontal (K^0_{hh}) and rocking (K^0_{rr}) degrees of freedom are considered.

For dynamic conditions, the dynamic impedance of foundation is written as

$$S_{ij}(\omega) = K_{ij}(\omega) + i\omega C_{ij}(\omega) \tag{2}$$

where K_{ij} and C_{ij} are the dynamic stiffness and damping, respectively, and i is the imaginary unit ($\sqrt{-1}$), which indicates a phase lag of 90º between the maximum spring force and the corresponding dashpot force. By employing the dimensionless frequency $a_0 = \omega B/V_s$, the dynamic impedance can be expressed as

$$S_{ij}(a_0) = K_{ij}^{0}\left[k_{ij}(a_0) + i\,a_0\,c_{ij}(a_0)\right] \tag{3}$$

where K^0_{ij} is the static stiffness and k_{ij}, c_{ij} are dimensionless stiffness and damping coefficients, respectively, as a function of the dimensionless frequency a_0. The dimensionless stiffness and damping coefficients are real-valued. It is noted that, whereas the k_{ij} coefficient may become negative at times (indicating a phase lag greater than 90º between excitation and response under dynamic conditions), c_{ij} is always positive so as to comply with thermodynamic constraints.

It is mentioned that parameter a_0 is essentially unique for halfspace conditions (where B is the only parameter carrying units of length), yet might not be so in the presence of bedrock at shallow depth [24], or in the presence of a significantly stiffer surface soil crust. For the interpretation of the present results, parameter $\omega h_1/V_{s1}$ was selected [25-26].

4 RESULTS FOR DYNAMIC STIFFNESS AND DAMPING

4.1 Results using cone model solutions

Fig. 2 presents results for the dimensionless static stiffness of a square rigid footing for both pre-liquefaction (V_{s1}/V_{s2}= 0.67 and 1.67) and post-liquefaction (V_{s1}/V_{sliq}= 4 and 10) con-

ditions. In the vertical axis, static stiffness is normalized with the shear modulus of the surface non-liquefiable soil crust ($G_1 = V_{s1}^2 \times \rho_1$) and the width of the footing (B) according to Eq. (1). Results are plotted against the thickness of the surface crust (h_1/B), for three values of h_2/B (= 0.5, 1, 2) parameter. The following noteworthy trends are evident [25-26]:

- The increase in the impedance contrast V_{s1}/V_{s2} leads to a significant decrease of the static stiffness coefficient, ranging from 28% to 78% for the vertical mode, 14% to 55% for the horizontal mode and 2% to 38% for the rocking mode.
- As the crust thickness ratio h_1/B increases, static stiffness coefficient for post-liquefaction case increases, which seems reasonable if one considers that for a thick top layer the pressure bulb beneath the loaded area (about 1.5 B in diameter) does not extend to the soft underlying liquefied soil.
- The variation in thickness of liquefied soil (h_2/B) seems to affect only marginally the static stiffness coefficient.

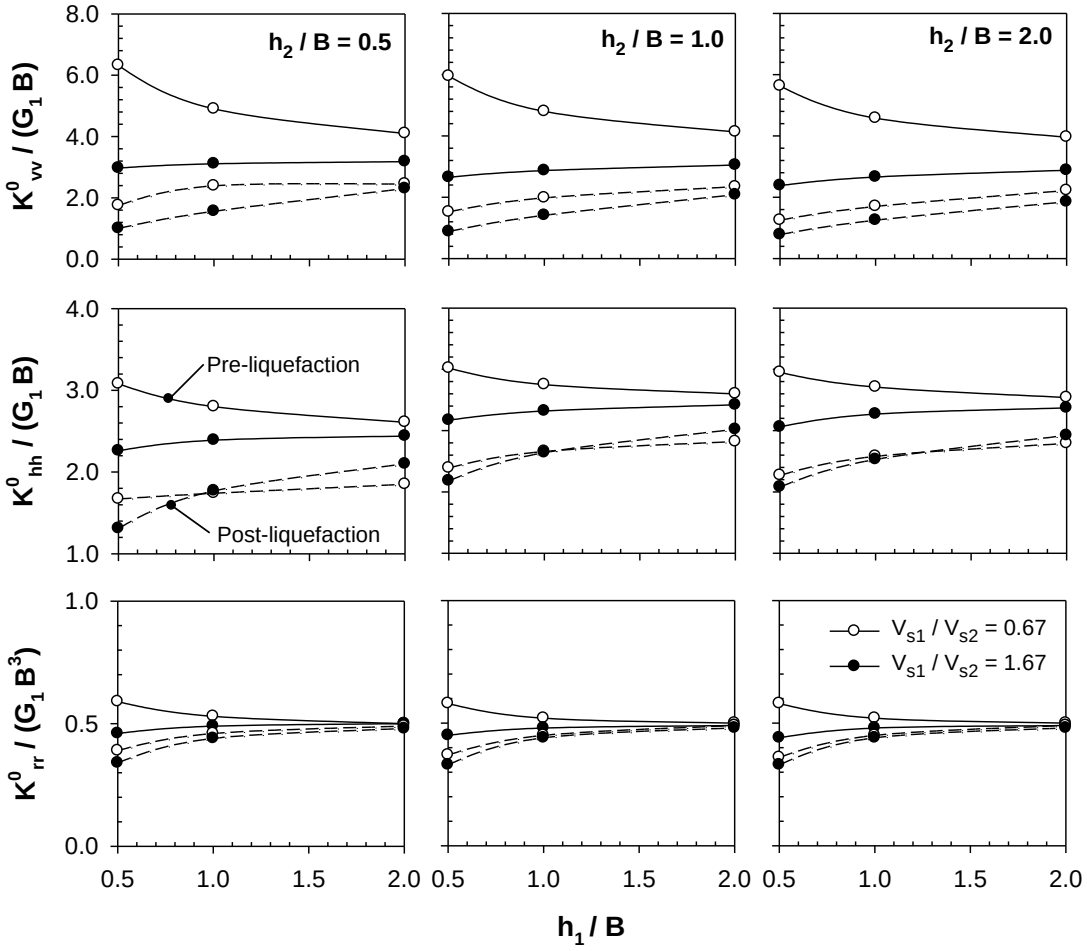

Figure 2: Normalized static stiffness of square rigid footing on three-layer liquefiable soil based on cone method.

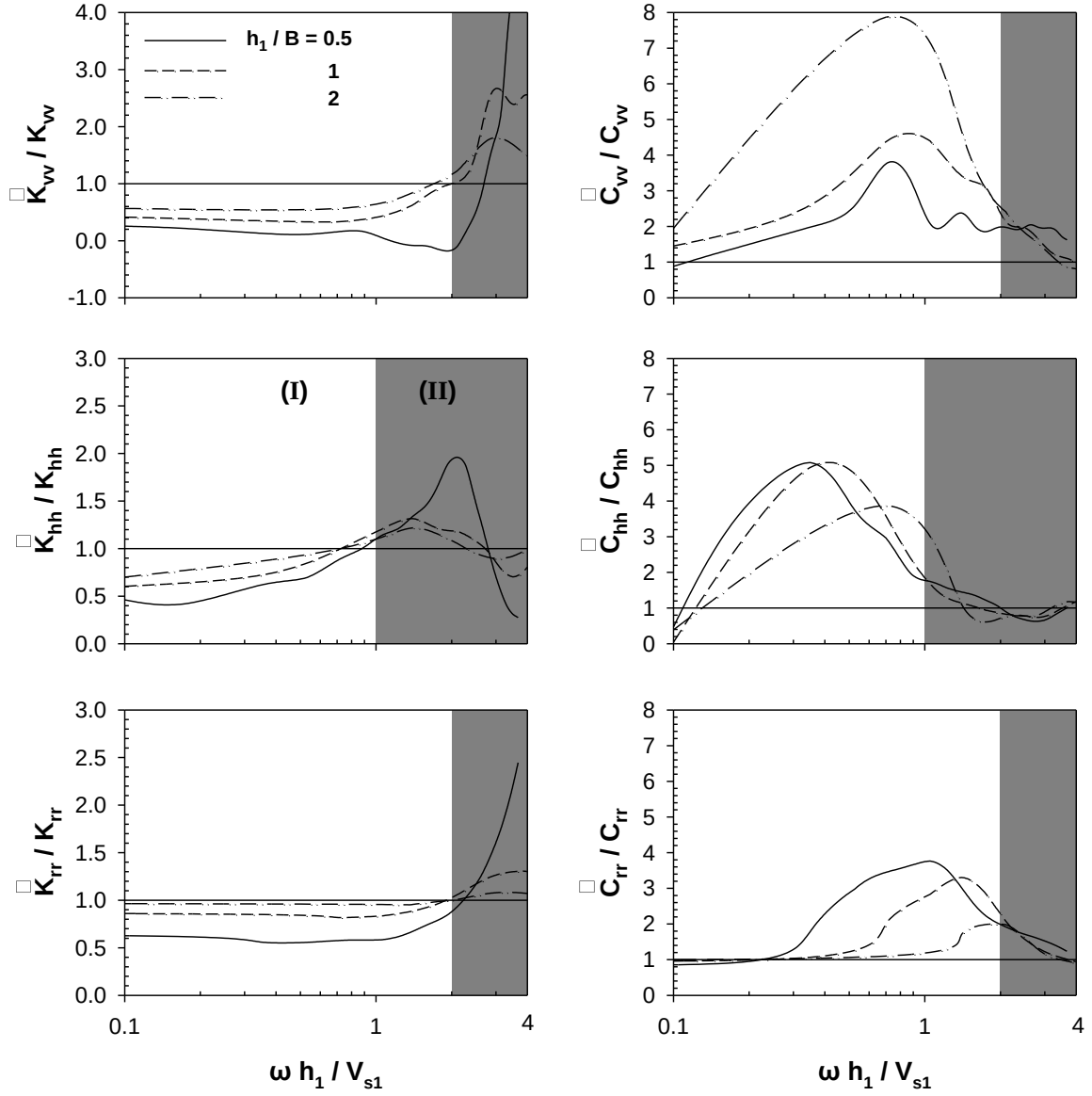

Figure 3: Normalized dynamic impedance functions of rigid square footing on liquefied soil for the three oscillation modes (vertical, horizontal, rocking). Effect of thickness of surface crust; $h_2/B = 1$, $V_{s1}/V_{s2} = 2/3$.

With reference to dynamic stiffness and damping, results are depicted in the form of dimensionless ratios $\tilde{K}_{ij} / K_{ij}$ and $\tilde{C}_{ij} / C_{ij}$ as a function of the dimensionless frequency $\omega h_1 / V_{s1}$ (Fig. 3). $\tilde{K}_{ij}$ and $\tilde{C}_{ij}$ denote the post-liquefied dynamic stiffness and damping, while K_{ij} and C_{ij} denote the pre-liquefied stiffness and damping values, respectively. The pertinent normalization scheme along with the logarithmic scale for the horizontal axis allow for a meaningful interpretation of the results. Fig. 3 shows typical results obtained by using the cone method. The following observations can be made [26]:

- Based on the variation of dynamic stiffness and damping ratios, two different regions in the graphs can be distinguished. For Region (I), the dynamic stiffness ratio $\tilde{K}_{ij} / K_{ij}$ decreases significantly while the corresponding damping ratio $\tilde{C}_{ij} / C_{ij}$ increases well above unity. For region (II), ratio $\tilde{K}_{ij} / K_{ij}$ seems to increase exhibiting sharp undulations while $\tilde{C}_{ij} / C_{ij}$ ratio tends to unity. This observation applies for all three oscillation modes.

- For vertical and rocking modes, the boundary between these two regions is located in $\omega h_1 / V_{s1} = 2$, and for horizontal mode in $\omega h_1 / V_{s1} = 1$.
- Region (I) refers to footings having small to moderate width, $B = 1 \sim 3$ m (h_1 is comparable to B), profiles with soft surface crust, $V_{s1} = 100 \sim 150$ m/s, and frequency range $f = 0 \sim 10$ Hz. On the other hand, region (II) corresponds to large width footings, $B > 4$ m, profiles with soft to moderate surface crust, $V_{s1} = 100 \sim 250$ m/s, and high frequency range $f > 15$ Hz. It is noteworthy that common buildings and structures fall into region (I).
- The variation in thickness of the surface crust has significant effect on the dynamic stiffness and damping coefficients. Specifically, as the h_1/B ratio decreases dynamic stiffness decreases in region (I). For region (II), h_1/B ratio does control the undulations in impedance functions.
- With reference to damping, a significant increase in post-liquefied damping is observed, mainly due to the increase in material damping of the liquefied layer. Increase in the thickness of the surface crust results in amplification of damping for the vertical mode, while the opposite trend is noticed for the other two modes. Interestingly, vertical damping coefficient exhibits a peak at around $\omega h_1 / V_{s1} \cong 0.75$, which suggests development of a kind of resonance at $T_{exc} \cong 2\ T_{s1}$ (i.e. $T_{s1} = 4h_1/V_{s1}$). However, this is not observed in the $\tilde{K}_{ij} / K_{ij}$ ratio.
- The variation in thickness of the liquefiable soil stratum (h_2/B), as well as in impedance contrast (V_{s1}/V_{sliq}) affects only slightly the dynamic impedance functions (not shown).
- Finally, at the high frequency range and for $h_1/B = 0.5$, dynamic stiffness coefficients are extremely high. It seems that the analysis with CONAN provides unstable solutions at the high frequency range and further investigation is required to produce robust results.

4.2 Comparison with BEM results

The comparison of the above results with those obtained by means of rigorous boundary element method is meaningful. For static stiffness in the post-liquefaction case, the maximum observed discrepancy is about 20%, while in the pre-liquefaction case the agreement is better with difference being less than 10% or so [26]. It is noted that BEM typically predicts higher values for static stiffness. The discrepancies, especially for the post-liquefaction case, are anticipated in light of the complexity of the problem and the extremely low value of shear wave velocity considered for the liquefied stratum ($V_{sliq} = 25$ m/s). However, both methods highlight the significant loss of stiffness of the foundation during liquefaction, with the percentage of reduction in static stiffness being comparable in the two approaches.

Regarding dynamic stiffness and damping coefficients, a comparison between results obtained by means of two independent analyses, for a typical case ($h_1/B = 1$, $h_2/B = 1$ and $V_{s1}/V_{s2} = 4$), is given in Fig. 4. Spring coefficient $\tilde{k}_{ij}$ and dashpot coefficient $\tilde{c}_{ij}$ are plotted, in accordance to Eq. 3, against the dimensionless frequency a_0, i.e., $\omega R/V_{s1}$ with $R = B/\sqrt{\pi}$ being the equivalent circular radius, stemming from the cone solution, and $\omega(B/2)/V_{s1}$ for results obtained using the boundary element method. It is observed that the agreement between Cone model predictions and BEM results is quite good.

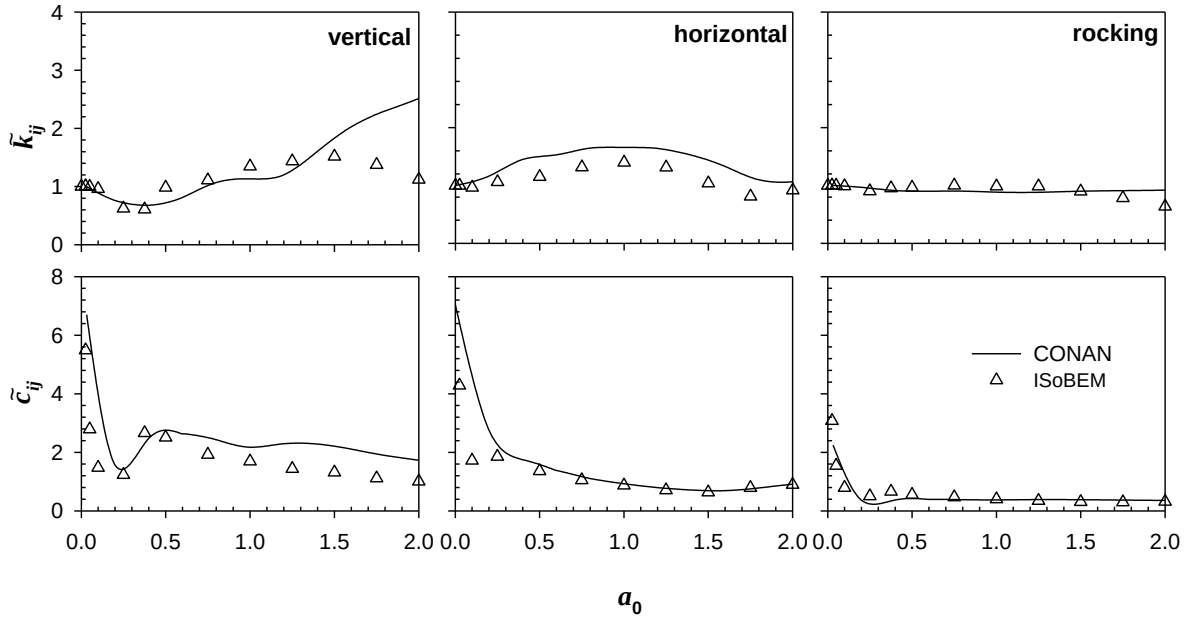

Figure 4: Comparison between cone model and BEM results for dynamic stiffness and damping coefficients; $h_1/B = 1$, $h_2/B = 1$, $V_{s1}/V_{s2} = 4$.

5 REGRESSION FORMULAE FOR STATIC STIFFNESS USING BEM RESULTS

A key objective of the paper is to develop regression formulae for the static stiffness of footings on liquefiable soil. Rigorous analyses using ISoBEM are performed to this end. The dimensionless ratios h_1/B = 0.5, 1, 2, h_2/B = 0.5, 1, 2, V_{s1}/V_{sliq} = 4, 7, 10, are examined. It is noted that, in the present analyses, for achieving better regression, the intermediate value V_{s1}/V_{sliq} = 7 is additionally investigated. All properties of the soil layers remain the same, with the exception of Poisson's ratio ν, being 0.499 for the second and third layer. No difference in the results due to those changes is observed.

5.1 Convergence and accuracy of BEM analysis

In the realm of BEM formulation, convergence studies for analyzing foundation impedance problems and dynamic soil-structure interaction have been conducted by several researchers [13, 27]. The most significant factors in providing accurate solutions are the distance of the non-reflecting truncation boundary and the boundary element size [28]. To select the optimum model of the pertinent problem, which will provide accurate results and computational efficiency, various 3D models (half and quarter domain) and mesh sizes for each oscillation mode were examined.

Taking advantage of the symmetry of geometry and loading, for the vertical (symmetric) oscillation mode, only one quarter of the system is analyzed. For the horizontal and rocking modes (antisymmetric), analyzing a half model is essential. To this end, the footing surface and the region around the footing up to a distance 3B is discretized using isoparametric four-noded quadrilateral linear elements with element length about 1/12 of the shear wavelength. Moreover, the surface beyond this region up to a distance of 5B needs fine mesh (element length = 1/8 of shear wavelength). The same also applies for the first interface (between first and second layer). In addition, discretization of the ground surface and the interfaces up to a distance of at least 10B to 15B beyond the foundation is necessary for obtaining accurate results. Coarser elements with lengths of about 1/3 to 1/2 of the shear wavelength are adequate for distant points [13].

For the vertical and horizontal oscillation mode, a uniform unit vertical and horizontal displacement, respectively, is applied to all element nodes of the footing and the resulting load is computed from the tractions developed on the element nodes [25]. For the rocking mode, a unit rotation is applied.

Because of lack of solutions for stiffness of square footings on three-layer soil profiles, the reliability of the models was checked a) by applying to all soil layers the same properties to obtain the stiffness of a rigid square footing on a halfspace, and b) by applying to the second and third layer the same properties, forming a two-layer soil profile, and comparing the results for stiffness with corresponding results in literature.

To establish the accuracy of the present BEM analysis, comparative studies are conducted with available published results. Table 1 provides the comparison of ISoBEM results for normalized static stiffness of rigid square footing on halfspace, for all three oscillation modes, with the empirical formulas from Pais & Kausel [7]. In Table 2, results for the horizontal static stiffness of a two-layer soil profile ($v_1 = v_2 = 0.4$) are compared against those obtained from Ahmad & Rupani [13]. Fig. 5 depicts the comparison of ISoBEM results for horizontal, vertical and rocking impedance of a square footing resting on a uniform soil layer over a halfspace ($V_{s1}/V_{s2} = 0.8$, $H/(B/2) = 1$, $v_1 = v_2 = 0.33$, $\rho_2/\rho_1 = 1.13$, $\beta_1 = 0.05$, $\beta_2 = 0.03$) with those reported by Wong and Luco [6]. Evidently, results obtained by analyzing the developed model in ISoBEM are in reasonable agreement with the published results.

Oscillation mode	[7]	ISoBEM	Difference (%)
Vertical (m=1)	7.12	6.93	2.7
Horizontal (m=1)	5.75	5.64	1.9
Rocking (m=3)	6.67	6.92	-3.7

Table 1: Comparison of normalized static stiffness $K^0_{ij}/(G_1B^m/2)$ of a rigid square footing on halfspace.

H/B/2	$V_{s1}/V_{s2} = 0.5$			$V_{s1}/V_{s2} = 2$		
	ISoBEM	[13]	Diff. (%)	ISoBEM	[13]	Diff. (%)
1	7.73	7.9	-2.2	3.79	3.8	-0.3
2	6.75	6.8	-0.7	4.50	4.4	2.2
4	6.22	6.2	0.3	5.09	5.0	1.8

Table 2: Comparison of normalized horizontal static stiffness $K^0_{hh}/(G_1B/2)$ of a rigid square footing on a two-layer soil profile.

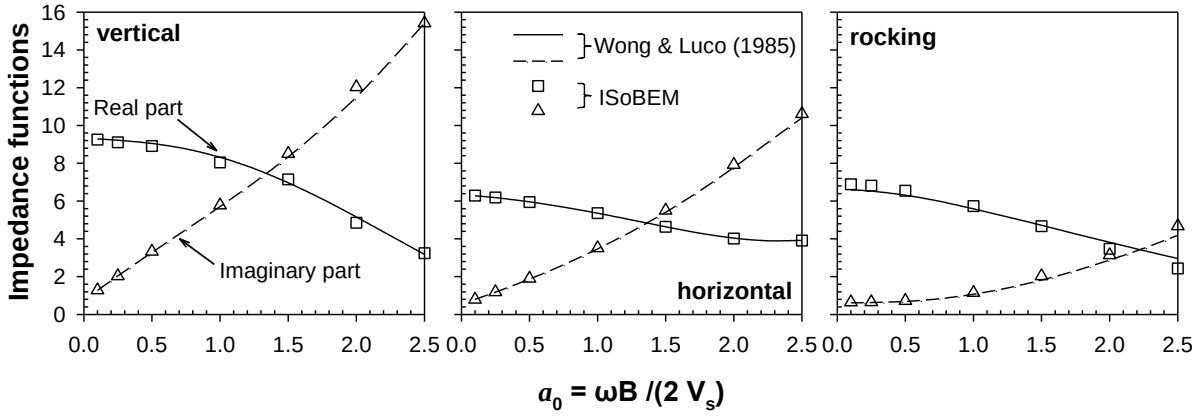

Figure 5: Comparison of vertical, horizontal and rocking dynamic stiffness coefficients of a square footing resting on a two-layer soil profile.

5.2 Numerical results and regression equations

Results for the static stiffness ratio $\tilde{K}^0_{ij}/K^0_{ij}$ obtained by means of ISoBEM, for all three degrees of freedom, are presented in Table 3. The outcome of this rigorous analysis is in meaningful agreement with the preliminary results obtained by using cone method and demonstrates the significant loss of stiffness upon liquefaction. Although results have been discussed in the previous section, it is worth mentioning that:

- The decrease ranges from 11% to 84% for the vertical mode, 11% to 56% for the horizontal and 1% to 59% for the rocking mode, being comparable with these predicted from the cone analyses.
- The highest decrease occurs in case of a very thin surface clay crust (h_1/B = 0.5) overlying a thick liquefiable sandy layer (h_2/B = 2), while the lowest decrease is observed in the opposite case, where a thin liquefiable sandy layer (h_2/B = 0.5) underlying a thick surface clay zone (h_1/B = 2).
- An important outcome of this investigation is that for a given set of h_1/B and h_2/B ratios the percentage of decrease is about the same regardless of V_{s1}/V_{sliq} ratio, which was not obvious in the preliminary results.
- With respect to horizontal mode, it is noted that the thickness of liquefiable soil layer appears to not affect substantially the horizontal stiffness.
- Regarding rocking mode, BEM results reveal a greater reduction in static stiffness in comparison with cone results, especially for h_1/B = 0.5, while in case of h_2/B = 2, the reduction is negligible.

Fig. 6 depicts the variation of normalized static stiffness of the footing in the post-liquefaction case with the thickness of the improved surface crust h_1/B, for three values of the liquefied soil zone h_2/B. Based on these numerical results, an attempt was made for developing regression equations for the static stiffness of a footing on liquefied soil. Using non-linear regression analysis in the results of Fig. 6, the following predictive equations are derived:

Vertical static stiffness

For h_2/B = 0.5,

$$\frac{K^0_{vv}}{G_1 B} = -0.28 + 8.34e^{-0.33\frac{V_{s1}}{V_{sliq}}} + \left(1 - e^{-1.2\frac{h_1}{B}}\right)\left[-6.82 + 10.15\left(1 - e^{-0.54\frac{V_{s1}}{V_{sliq}}}\right)\right] \quad (4)$$

For $1 \le h_2/B \le 2$,

$$\frac{K_{vv}^0}{G_1 B} = \left(1.54 - 0.27\frac{h_2}{B}\right)\left\langle\left(-0.174 + 2.33e^{-0.254\frac{V_{s1}}{V_{sliq}}}\right) + \left\{\left(2.24 + 2.84\frac{h_2}{B}\right)\left[1 - e^{-\left(0.72 - 0.21\frac{h_2}{B}\right)\frac{h_1}{B}}\right] - \left(2.04 - 0.15\frac{h_2}{B}\right)\left[1 - e^{-\left(0.05 + 0.46\frac{h_2}{B}\right)\frac{h_1}{B}}\right]\right\}\right\rangle \quad (5)$$

Horizontal static stiffness

$$\frac{K_{hh}^0}{G_1 B} = \left[1.07 - 0.18\frac{h_2}{B} + 0.07\left(\frac{h_2}{B}\right)^2\right] \times \left\langle\left(0.32 + 2.46 \times e^{-0.32\frac{V_{s1}}{V_{sliq}}}\right) + 2.1 \times \left(1 - e^{-0.55\frac{V_{s1}}{V_{sliq}}}\right)\left\{1 - e^{-\frac{h_1}{B}\left[2.02 - 0.83\left(\frac{h_2}{B}\right)^{0.45}\right]}\right\}\right\rangle \quad (6)$$

Rocking static stiffness

$$\frac{K_{rr}^0}{G_1 B^3} = 0.01 + \frac{1}{1.26 + 0.006\left(V_{s1}/V_{sliq}\right)}\left\{1 - e^{-\left(\frac{1}{0.37 + 0.024\,V_{s1}/V_{sliq}} - \frac{1}{1.68 + 0.28\,V_{s1}/V_{sliq}}\frac{h_2}{B}\right)\frac{h_1}{B}}\right\} \quad (7)$$

The above equations can be used in applications as a preliminary assessment of the problem. It is noted that the regression formulae are valid for the post-liquefaction case, i.e., $V_{s1}/V_{sliq} > 1$, and for the parameter range examined in the analyses i.e., $0.5 \le h_2/B \le 2.0$. Numerical values obtained from the regression formulae are illustrated in Fig. 6.

		$\tilde{K}^0_{ij}/K^0_{ij}$								
		Vertical			Horizontal			Rocking		
		V_{s1}/V_{sliq}								
h_1/B	h_2/B	4	7	10	4	7	10	4	7	10
0.5	0.5	0.41	0.38	0.39	0.54	0.52	0.54	0.53	0.53	0.55
	1	0.25	0.24	0.26	0.48	0.48	0.52	0.46	0.45	0.48
	2	0.17	0.16	0.17	0.44	0.45	0.50	0.42	0.41	0.44
1	0.5	0.68	0.64	0.64	0.74	0.70	0.71	0.88	0.87	0.88
	1	0.51	0.47	0.47	0.69	0.66	0.69	0.85	0.83	0.85
	2	0.36	0.32	0.33	0.64	0.63	0.67	0.81	0.82	0.82
2	0.5	0.89	0.87	0.87	0.89	0.86	0.86	0.99	0.99	0.99
	1	0.80	0.77	0.76	0.85	0.83	0.84	0.97	0.97	0.97
	2	0.68	0.63	0.63	0.81	0.81	0.83	0.96	0.97	0.99

Table 3: Post-liquefied static coefficient of square footing normalized with the corresponding pre-liquefied static coefficient.

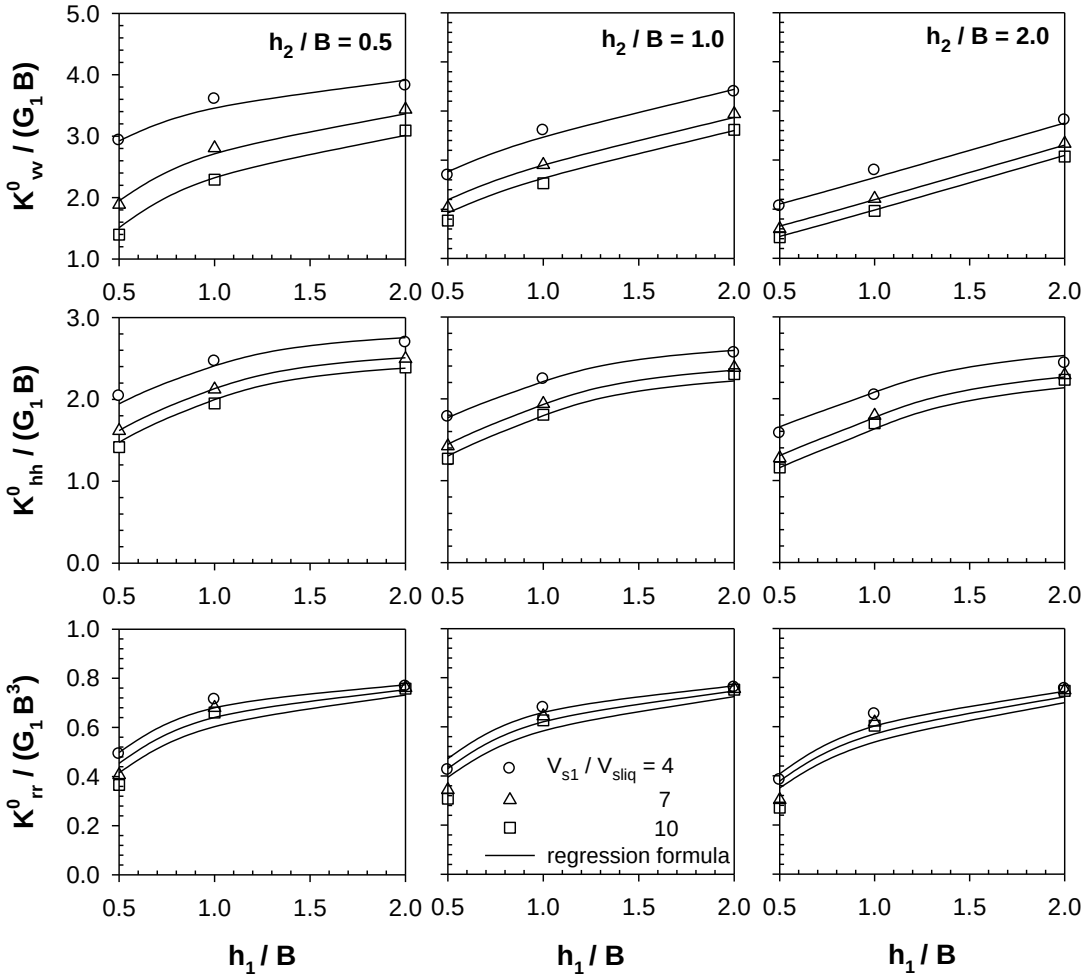

Figure 6: Normalized static stiffness of square rigid footing on liquefied soil based on BEM results and results obtained using regression formulae.

6 CONCLUSIONS

Under the convenient assumption of equivalent material linearity, the dynamic impedance problem of a rigid footing lying on a three-layer liquefiable soil profile was numerically investigated, considering all three planar oscillation modes (vertical, horizontal and rocking). Notwithstanding the non-linear nature of the liquefaction phenomenon, it was shown that one may employ elastodynamic analysis as an engineering approach to the problem in the sub-structuring sense, assuming appropriate values for the shear wave velocity and material damping of the liquefied soil stratum, and considering a kind of "permanent" liquefied condition during the seismic event.

The dynamic impedance of the footing was evaluated for both pre-and post-liquefaction conditions so as to highlight the impact of liquefaction. Numerical results from both simplified cone models and rigorous BEM analyses have demonstrated a significant reduction in footing stiffness along with a considerable increase in overall damping owing to liquefaction. Among the parameters explored, the thickness of the surface non-liquefiable soil layer is the one that seems to control the change in dynamic stiffness and damping.

Based on the boundary element results, regression formulae for the vertical, horizontal and rocking static stiffness were obtained, which can be used for an initial assessment of the static stiffness of a surface foundation on liquefied soil.

ACKNOWLEDGEMENTS

This research was co-financed by the European Union (European Social Fund – ESF) and Greek national funds through the Operational Program "Education and Lifelong Learning" of the National Strategic Reference Framework (NSRF)-Research Funding Program: THALES. Investing in knowledge society through the European Social Fund. The help of Professors Demosthenes Polyzos and Dimitri Beskos of UPatras in making available ISoBEM software to the authors is gratefully acknowledged, as well as the help of Professor Stephanos Tsinopoulos of the Technological Institute of Patras in using the software.

REFERENCES

[1] Karamitros, G. Bouckovalas, Y. Chaloulos, Insight into the seismic liquefaction performance of shallow foundations. *Journal of Geotechnical and Geoenvironmental Engineering*, **139**, 599-607, 2013 (a).

[2] D. Karamitros, G. Bouckovalas, Y. Chaloulos, Seismic settlements of shallow foundations on liquefiable soil with a clay crust. *Soil Dynamics and Earthquake Engineering*, **46**, 64-76, 2013(b).

[3] D. Karamitros, G. Bouckovalas, Y. Chaloulos, K. Andrianopoulos, Numerical analysis of liquefaction-induced bearing capacity degradation of shallow foundations on a two-layered soil profile. *Soil Dynamics and Earthquake Engineering*, **44**, 90-101, 2013(c).

[4] A. Acacio, Y. Kobayashi, I. Towhata, R. Bautista, K. Ishihara, Subsidence of building foundation resting upon liquefied subsoil; Case studies and assessment. *Soils and Foundations*, **41**(6), 111-128, 2001.

[5] N. Sitar, E. Hausler, Influence of Ground Improvement on Liquefaction Induced Settlements: Observations from Case Histories and Centrifuge Experiments. *Invited Lecture presented to the Korean Geotechnical Society*, Seoul, Korea, March 22, 2012.

[6] HL. Wong, JE. Luco, Tables of impedance functions for square foundation on layered media. *Soil Dynamics and Earthquake Engineering*, **4**(2),64–81, 1985.

[7] A. Pais, E. Kausel, Approximate formulas for dynamic stiffnesses of rigid foundations. *Soil Dynamics and Earthquake Engineering*, **7**(4), 213–227, 1988.

[8] G. Gazetas, Formulas and charts for impedances of surface and embedded foundations. *Journal of Geotechnical Engineering*, **117** (9), 1363-1381, 1991.

[9] JW Meek, JP. Wolf, Cone models for soil layer on rigid rock. *Journal of Geotechnical Engineering, ASCE*, **118**, 686–703, 1992.

[10] J.P. Wolf, *Foundation vibrations analysis using simple physical models*. Prentice Hall, 1994.

[11] C. Vrettos, Vertical and rocking impedances for rigid rectangular foundations on soils with bounded non-homogeneity. *Earthquake Engineering and Structural Dynamics*, **28** (12), 1525-1540, 1999.

[12] G. Mylonakis, S. Nikolaou, G. Gazetas, Footings under seismic loading: Analysis and design issues with emphasis on bridge foundations. *Soil Dynamics and Earthquake Engineering*, **26** (9), 824-853, 2006.

[13] S. Ahmad, A. Rupani, Horizontal impedance of square foundation in layered soil. *Soil Dynamics and Earthquake Engineering*, **18**(1), 59-69, 1999.

[14] NIST, *Soil-Structure Interaction for Building Structures*, GCR 12-917-21, prepared by the NEHRP Consultants Joint Venture, a partnership of the Applied Technology Council and the Consortium for Universities for Research in Earthquake Engineering, for the National Institute of Standards and Technology, Gaithersburg, MD, 2012.

[15] S. Miwa, T. Ikeda, Shear modulus and strain of liquefied ground and their application to evaluation of the response of foundation structures. *Structural Engineering/Earthquake Engineering, JSCE*, **23** (1), 167-179, 2006.

[16] A. Theocharis, Numerical analysis of liquefied ground response under harmonic seismic excitation-Variable thickness of liquefied layer. *Diploma thesis*, NTUA, Greece. 2011.

[17] E. Buckingham, On physically similar systems; illustrations of the use of dimensional equations. *Physical Review*, **4** (4), 345-376, 1914.

[18] J.P. Wolf, A.J. Deeks, *Foundation Vibration Analysis: A Strength-of-Materials Approach*. Elsevier, Oxford, UK, 2004.

[19] D. Hiltunen, P. Dunn, U. Toros, Cone model predictions of dynamic impedance functions of shallow foundations. *4th International Conference on Earthquake Geotechnical Engineering ICEGE*, Thessaloniki, Greece, 2007.

[20] ISoBEM: *Boundary Element Method Package*. http://bemsands.com, 2012.

[21] D. Polyzos, S. Tsinopoulos, D. Beskos, Static and dynamic boundary element analysis in incompressible linear elasticity. *European Journal of Mechanics A/Solids*, **17** (3), 515-536, 1998.

[22] S. Tsinopoulos, S. Kattis, D. Polyzos, D. Beskos, An advanced boundary element method for axisymmetric elastodynamic analysis, *Computer Methods in Applied Mechanics and Engineering*, **175**, 53-70, 1999.

[23] B. Heidarzadeh, G. Mylonakis, JP. Stewart, Stresses beneath dynamically applied vertical point loads. *6th International Conference on Earthquake Geotechnical Engineering ICEGE*, Christchurch, New Zealand, 2015.

[24] G. Anoyatis, G. Mylonakis, Dynamic Winkler modulus for axially loaded piles. *Geotechnique*, **62**, 521-536, 2012.

[25] X. Karatzia, *Theoretical investigation of geotechnical seismic isolation of bridge piers on footings and piles*. Doctoral Dissertation, Department of Civil Engineering, University of Patras, Greece, 2016.

[26] X. Karatzia, G. Mylonakis, G. Bouckovalas, 3D Dynamic impedances of surface footings on liquefiable soil: equivalent linear approach. *16th World Conference on Earthquake Engineering WCEE*, Santiago, Chile, 2017.

[27] S, Ahmad, A. Bharadwaj, Horizontal impedance of embedded strip foundations in layered soil. *Journal of Geotechnical Engineering*. **117**, 1021–41, 1991.

[28] C. C. Spyrakos, C. J. Xu, Dynamic analysis of flexible massive strip-foundations embedded in layered soils by hybrid BEM-FEM. *Computers & Structures*, **82**(29–30), 2541–2550, 2004.